Hygrothermal Modeling: a Numerical and Experimental Study on Drying

M. Bianchi Janetti[*1], F. Ochs[1], L. P. M. Colombo[2]
[1]Unit for Energy Efficient Buildings, University of Innsbruck
[2]Dipartimento di Energia, Politecnico di Milano, via Lambruschini 4, 20156 Milan, Italy
*Corresponding author: Technikerstr. 13, 6020 Innsbruck, Austria, michele.janetti@uibk.ac.at

Abstract: A model for coupled heat and mass transfer in porous, capillary-active materials is validated against experimental data obtained by drying calcium silicate specimens. The accuracy of the numerical solution is qualitatively investigated by considering mass conservation for a set of different cases, varying boundary conditions and numerical setup.
It is shown that the model is able to reproduce adequately the drying behavior. However, mass conservation is guaranteed just for proper numerical inputs, depending on the boundary conditions.

Keywords: heat and moisture transfer; capillary active materials; drying test; mass balance ratio

1. Introduction

The use of COMSOL in building-physics for hygrothermal modeling of materials and components is nowadays state of the art, as shown by numerous studies published in recent years e.g. [1], [2], [3], [4], [5], [6] and [7]. However, the majority of considered cases refer to heat and moisture transfer in hygroscopic range (relative humidity below ca. 98%) while it has been shown that modeling the material behavior in the super hygroscopic range (relative humidity up to 100%) may represent a numerical challenge [3]. This is due to the fact that the material functions (in particular the water storage function and the liquid water diffusivity) are in general highly non-linear at saturation and the numerical errors may become important in that range.

This paper aims at handling this challenge, by considering drying tests performed on calcium silicate specimens. Simulation results obtained through 3D modelling of laboratory experiments are compared with measured data. Moreover, considerations on the numerical quality of the solutions are made. The preliminary results are very promising for a further application of COMSOL for hygrothermal simulation in the super hygroscopic range. Indeed, numerical parameters and boundary conditions may have important impact on the accuracy of the numerical solution.

2. Experiment description

Drying tests have been performed inside a climatic chamber under controlled boundary conditions (temperature and relative humidity) for a set of calcium silicate specimens (Figure 1, left). The experiment starts with saturated specimens, which are dried until equilibrium with the surrounding air is reached.
Mixed convection occurs inside the chamber since the air velocity is influenced on the one hand by the difference between surface and air temperature, on the other hand by the fan operation.
All the specimen surfaces are in contact with the surrounding air and three symmetry planes can be defined, hence, only an eighth of the specimen has been reproduced for numerical simulation (Figure 1, right).
The water contents and drying rates are determined by weighting the specimens at different times, while the surface temperature is measured through infrared thermography.

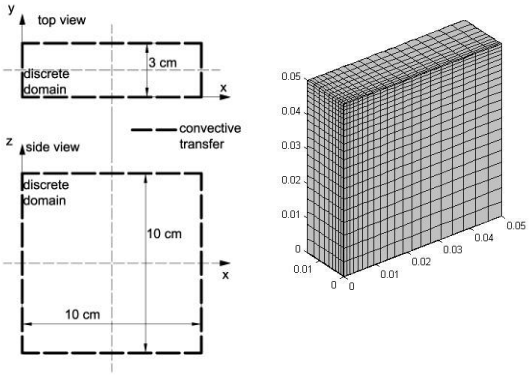

Figure 1: schematic of the drying specimen with three symmetry planes (left) and mesh (right, dimensions in meters)

3. Governing Equations and Use of COMSOL Multiphysics®

According to a widespread approach [8], the heat and moisture transfer processes in the porous domain is described by the following driving equations:

$$\frac{\partial H}{\partial T}\frac{\partial T}{\partial t}+\frac{\partial H}{\partial \varphi}\frac{\partial \varphi}{\partial t}=\nabla\cdot(K_{11}\nabla T+K_{12}\nabla\varphi) \quad (1)$$

$$\frac{\partial u}{\partial \varphi}\frac{\partial \varphi}{\partial t}=\nabla\cdot(K_{21}\nabla T+K_{22}\nabla\varphi) \quad (2)$$

With the boundary conditions given by Equations (3) and (4):

$$\begin{aligned}(K_{11}\nabla T+K_{12}\nabla\varphi)\cdot\boldsymbol{n}&=\alpha[T_\infty-T(\boldsymbol{x},t)]\\&+h_v\beta[p_s(T_\infty)\varphi_\infty\\&-p_s(T(\boldsymbol{x},t))\varphi(\boldsymbol{x},t)]\end{aligned} \quad (3)$$

$$\begin{aligned}(K_{21}\nabla T+K_{22}\nabla\varphi)\cdot\boldsymbol{n}&=\beta[p_s(T_\infty)\varphi_\infty\\&-p_s(T(\boldsymbol{x},t))\varphi(\boldsymbol{x},t)]\end{aligned} \quad (4)$$

Equations (1) to (4) are implemented in Comsol using the "coefficient form PDE" and defining the transfer coefficients K_{ij} as follows:

$$K_{11}=-\lambda-\left(h_{lv}+c_{p,v}\theta\right)\frac{\varphi D_v}{\mu R_v T}\frac{dp_s}{dT} \quad (5)$$

$$K_{12}=-\left(h_{lv}+c_{p,v}\theta\right)\frac{p_s D_v}{\mu R_v T}-c_w\theta D_w\frac{\partial u}{\partial\varphi} \quad (6)$$

$$K_{21}=-\frac{\varphi D_v}{\mu R_v T}\frac{dp_s}{dT} \quad (7)$$

$$K_{22}=-\frac{p_s D_v}{\mu R_v T}-D_w\frac{\partial u}{\partial\varphi} \quad (8)$$

All symbols concerning transfer equations and boundary conditions are listed in the nomenclature.

The material functions characterizing the hygrothermal behavior of calcium silicate, determined in previous studies (e.g. [9]), are shown in Figure 2.

Note that the equations (1) and (2) lead to a mass conservation error if implemented in Comsol. This is due to the fact that the damping coefficient $du/d\varphi$ in equation (2) depends strongly on the variable φ [10], [11]. This error, however, may be acceptable if adequate numerical measures are employed [12], [3].

The drying process represents a challenging test for evaluating the numerical performance since at saturation water retention curve and liquid water diffusivity are highly non-linear. Moreover different moisture transfer mechanisms, such as vapor diffusion and capillary transfer, are superimposed during drying. These issues may lead to difficulties which require adequate numerical setup, as shown later on in the paper.

In Table 1 the parameters used for the simulation are reported.

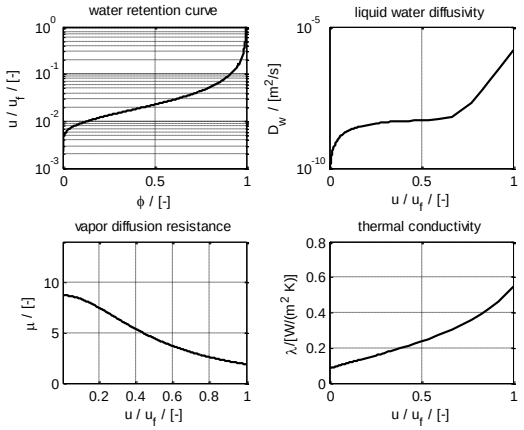

Figure 2: material functions of calcium silicate according to [9] (max. water content: u_f=852 [kg/m^3])

Table 1: Numerical setup

Parameter	Value / Setup
Mesh elements	4000
Element ratio	5
Shape function	Lagrange
Element order	linear
Absolute tolerance	10^{-5}
Relative tolerance	10^{-4}
Time step	variable
Time stepping method	BDF
Max. BDF order	5

4. Results

The experiment is repeated for a set of boundary conditions, defined in Table 2, which produce different drying rates. The measured data are then compared with the model results.

In Figure 3 the time trends of total water content and drying rate are reported, while in Figure 4 the mean temperature difference between surface and air, as well as the mean

relative humidity at the specimen surface are shown.

It can be observed that the model is able to reproduce adequately the drying behavior. In particular, the temperature reduction due to evaporation cooling observed at the specimen surface is explained (Figure 4 left; measured values are available just for bc2).

Table 2: boundary conditions

case	θ∞ [°C]	φ∞ [-]	α [W/m2K]	β [s/m]
bc1	23.5	0.52	9.32	$2.86 \cdot 10^{-8}$
bc2	25.0	0.40	11.84	$4.51 \cdot 10^{-8}$
bc3	30.0	0.35	12.60	$8.31 \cdot 10^{-8}$

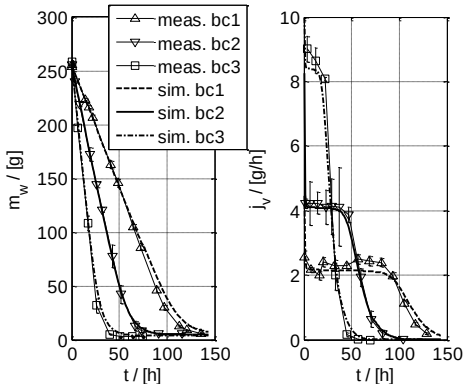

Figure 3: trends of the total water content inside the specimens (left); drying rates (right)

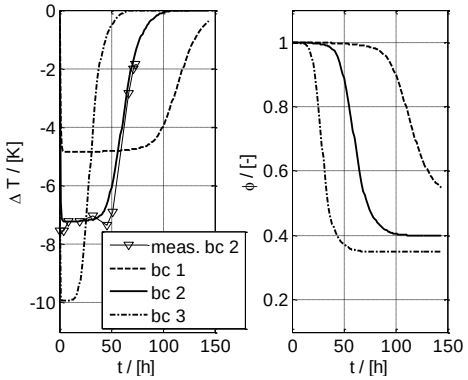

Figure 4: trends of the average temperature difference between air and surface (left); trend of mean relative humidity at the surface (right)

In Figure 5 the simulated surface temperature and relative humidity are shown at different times during drying for case bc2. The samples are drying first on the edges and later on in the center, revealing the 3D nature of the process.

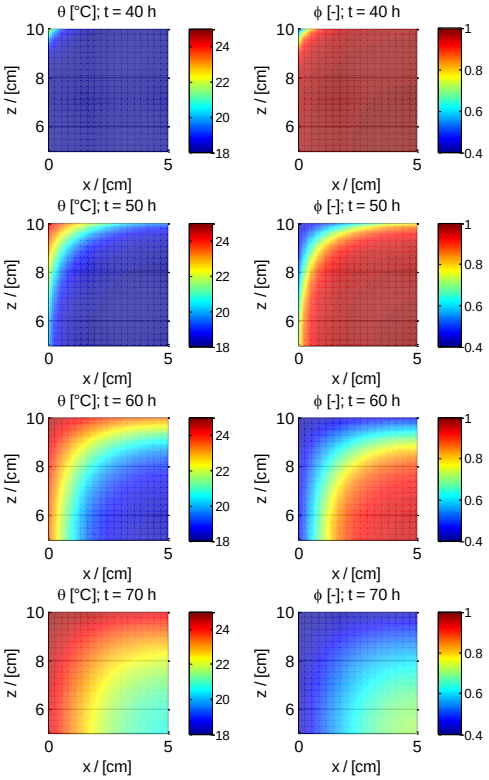

Figure 5: surface distributions of temperature and relative humidity at different times (plane y=0) for the case bc2 defined in Table 2.

In order to evaluate the quality of the numerical solution, we consider the mass balance ratio, defined as follows:

$$MB(t) = \frac{total\ mass\ loss}{total\ net\ flux\ from\ the\ domain}$$

This parameter gives a measure of the mass conservation errors affecting the simulation. Exactly conservative solutions correspond to a mass balance ratio equal to one at every time step, while poor numerical quality may lead to important deviations of this parameter.

In Figure 6 the results calculated with the numerical setup defined in Table 1 are reported.

It can be observed that the parameter MB depends strongly on the boundary conditions, i.e. faster drying reduces oscillations of this parameter. Moreover, main deviations occur in all cases around in the middle of the early drying period, which presents nearly constant drying rates.

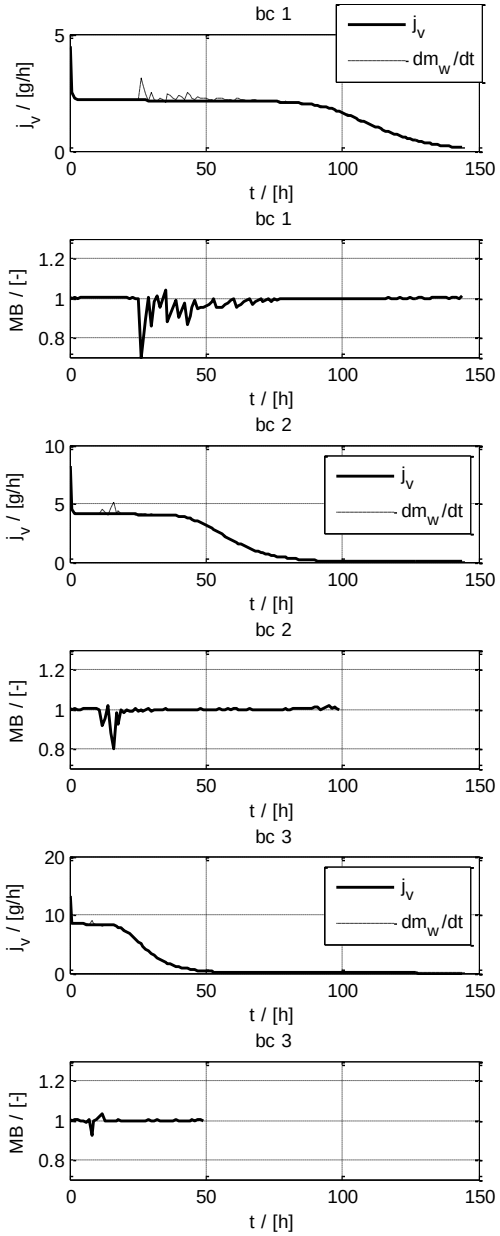

Figure 6: drying rates and mass balance ratios for the three considered cases defined in Table 2

A quantitative explanation of the mass balance ratio trend may be difficult, due to the complexity of the model. Such analysis would overcome the scope of this study. Here, we just consider qualitatively the influence of two input parameters, i.e. the absolute tolerance and number of mesh elements (Table 3), on the simulation results. To this aim, the parameter MB(t) is integrated over time and divided by the simulation time, obtaining a single value MB_{int}, which gives a measure of the total mass conservation error for each simulation.

In Figure 7 the values of MB_{int} are reported against the absolute tolerance (top) and number of mesh elements (bottom).

While important improving has been obtained by reducing the absolute tolerance, no significant difference has been observed by refining the mesh. It can be observed that, with an absolute tolerance of 10^{-5}, the total mass conservation error remains in all cases under 5%.

Table 3: number of mesh elements

Mesh	Number of elements			
	x	y	z	total
1	12	6	12	864
2	16	8	16	2048
3	20	10	20	4000
4	24	12	24	6900

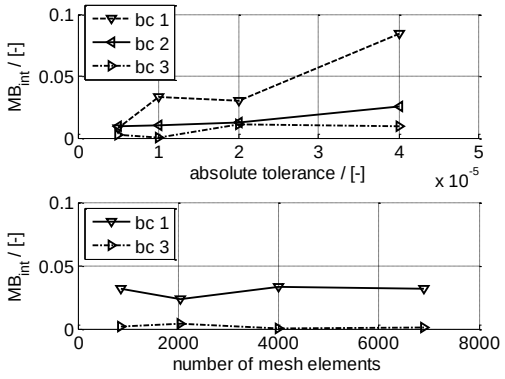

Figure 7: Parameter MB_{int} for different absolute tolerances (top) and number of elements (bottom). All other parameters are defined in Table 1

4. Conclusion and outlook

The complex phenomenon of drying capillary active materials is accurately reproduced through a 3D Model for coupled heat and mass transfer implemented using the "coefficient form PDE". Even if good agreement with experimental data is obtained, the numerical solution is not able to guarantee mass conservation. This limitation is qualitatively investigated by varying the numerical setup, i.e. mesh and absolute tolerance. The impact of the absolute tolerance on the solution is important. Setting a value of 10^{-5} for this parameter produces enough accurate solutions in all considered cases since the total mass

conservation error remains under 5%. However, this study has to be considered as a preliminary analysis. Further work is required in order to generalize the results, i.e. considering the influence of the other input parameters.

5. Acknowledgements

The authors kindly thank Renato Passaniti, Dominik Granig, Andreas Saxer and Markus O. Feichter for their support.

6. Nomenclature

c	$[J/(kg\ K)]$	*Heat capacity*
D	$[m^2/s]$	*Diffusivity*
j	$[kg/s]$	*Total mass flux*
K_{11}	$[W/(m\ K)]$	*Transport coefficients*
K_{12}	$[W/m]$	
K_{21}	$[kg/(m\ s\ K)]$	
K_{22}	$[kg/(m\ s)]$	
h	$[J/Kg]$	*Specific enthalpy*
H	$[J/m^3]$	*Volumetric enthalpy*
m	$[kg]$	*Mass*
MB	$[-]$	*Mass balance ratio*
$\boldsymbol{n}$	$[-]$	*Normal unit vector*
p	$[Pa]$	*Partial pressure*
R	$[J/(kg\ K)]$	*Gas constant*
t	$[s]$	*Time*
T	$[K]$	*Temperature*
u	$[kg/m^3]$	*Volumetric water content*
$x;y;z$	$[m]$	*Coordinates*
α	$[W/(m^2K)]$	*Heat transfer coefficient*
β	$[s/m]$	*Mass transfer coefficient*
θ	$[°C]$	*Temperature*
λ	$[W/m\ K]$	*Thermal conductivity*
μ	$[-]$	*Vapor diffusion resistance*
φ	$[\%]$	*Relative humidity*

Subscripts

f	*Free saturation*
w	*Liquid water*
p	*Constant pressure*
v	*Vapor*
s	*Saturation*
∞	*In the surrounding air*

6. References

[1] A. W. M. J. Van Schijndel, "Heat and Moisture Modeling Benchmarks using COMSOL," in *Comsol Conference Hannover*, 2008.

[2] A. W. M. van Schijndel, "Integrated modeling of dynamic heat, air and moisture processes in buildings and systems using SimuLink and COMSOL," *Build. Simul.*, vol. 2, pp. 143–155, 2009.

[3] M. Bianchi Janetti, F. Ochs, and W. Feist, "Numerical Quality of a Model for Coupled Heat and Moisture Transport in COMSOL Multiphysics," *2nd Cent. Eur. Symp. Build. Physics, Vienna*, 2013.

[4] L. Nespoli, M. Bianchi Janetti, and F. Ochs, "Comparing Different Approaches for Moisture Transfer inside Constructions with Air Gaps," in *Comsol Conference Rotterdam*, 2013.

[5] J. I. Knarud and S. Geving, "Implementation and Benchmarking of a 3D Hygrothermal Model in the COMSOL Multiphysics Software," *Energy Procedia*, vol. 78, no. 1876, pp. 3440–3445, 2015.

[6] M. Teibinger, "Coupled Heat and Moisture Transfer in Building Components - Implementing WUFI Aproaches in COMSOL Multiphysics," in *Comsol Conference Milano*, 2012.

[7] A. Ozolins, A. Jakovics, and A. Ratnieks, "Moisture Risks in Multi-layered Walls - Comparison of COMSOL Multiphysics ® and WUFI ® PLUS Models with Experimental Results," in *Comsol Conference Rotterdam*, 2013.

[8] H. Künzel and K. Kiessl, "Calculation of heat and moisture transfer in exposed building components," *Int. J. Heat Mass Transf.*, vol. 40, no. 1, pp. 159–167, Oct. 1996.

[9] M. Bianchi Janetti, T. A. Carrubba, F. Ochs, and W. Feist, "Heat flux measurements for determination of the liquid water diffusivity in capillary active materials," *Int. J. Heat Mass Transf.*, vol. 97, pp. 954–963, 2016.

[10] M. Celia, E. Bouloutas, and R. Zarba, "A general mass-conservative numerical solution for the unsaturated flow equation," *Water Resour. Res.*, vol. 26, no. 7, pp. 1483–1496, 1990.

[11] H. Janssen, B. Blocken, and J. Carmeliet, "Conservative modelling of the moisture and heat transfer in building components under atmospheric excitation," *Int. J. Heat Mass Transf.*, vol. 50, no. 5–6, pp. 1128–1140, Mar. 2007.

[12] M. Bianchi Janetti, F. Ochs, and W. Feist, "On the conservation of mass and energy in hygrothermal numerical simulation with COMSOL Multiphysics," *Build. Simul. Conf. Chambery*, 2013.